Engineering zonal cartilaginous tissue by modulating oxygen levels and mechanical cues through the depth of infrapatellar fat pad stem cell laden hydrogels.

Luo, L; O'Reilly, AR; Thorpe, SD; Buckley, CT; Kelly, DJ

Engineering zonal cartilaginous tissue by modulating oxygen levels and mechanical cues through the depth of infrapatellar fat pad stem cell laden hydrogels

Engineering zonal cartilaginous tissue by modulating oxygen levels and mechanical cues through the depth of infrapatellar fat pad stem cell laden hydrogels

Lu Luo [a,b], Adam R. O'Reilly [a,b], Stephen D. Thorpe [c], Conor T. Buckley [a,b], Daniel J. Kelly [a,b,d,e]∗

[a] Trinity Centre for Bioengineering, Trinity Biomedical Sciences Institute, Trinity College Dublin, Dublin, Ireland.

[b] Department of Mechanical and Manufacturing Engineering, School of Engineering, Trinity College Dublin, Dublin, Ireland.

[c] Institute of Bioengineering, School of Engineering and Materials Science, Queen Mary University of London, London, UK.

[d] Department of Anatomy, Royal College of Surgeons in Ireland, Dublin 2, Ireland.

[e] Advanced Materials and Bioengineering Research Centre (AMBER), Royal College of Surgeons in Ireland and Trinity College Dublin, Dublin, Ireland.

∗Corresponding author

E-mail address: kellyd9@tcd.ie

Address: Department of Mechanical and Manufacturing Engineering

School of Engineering

Trinity College Dublin

Dublin 2

Ireland

Telephone: +353-1-896-3947

Fax: +353-1-679-5554

Abstract

Engineering tissues with a structure and spatial composition mimicking those of native articular cartilage (AC) remains a challenge. This study examined if infrapatellar fat pad derived stem cells (FPSCs) can be used to engineer cartilage grafts with a bulk composition and a spatial distribution of matrix similar to the native tissue. In an attempt to mimic the oxygen gradients and mechanical environment within AC, FPSC laden hydrogels (either 2mm or 4mm in height) were confined to half of their thickness and subjected to dynamic compression (DC). Confining hydrogels was predicted to lower the oxygen tension in the bottom of constructs, increasing both total glycosaminoglycan (GAG) and collagen synthesis in 2mm high tissues. When subjected to DC alone, both GAG and collagen accumulation increased within these constructs. Furthermore, the dynamic modulus of constructs increased from 0.96 MPa to 1.45 MPa. In contrast, there was no beneficial effect of either confinement or DC on tissue development of 4mm high constructs. Furthermore, there was no synergistic benefit of coupling confinement and DC on overall levels of matrix accumulation; however in all constructs, irrespective of their height, the combination of these boundary conditions lead to the development of engineered tissues that spatially best resembled native AC. The superficial region of these constructs mimicked that of native tissue, staining weakly for GAG, strongly for type II collagen, and in 4mm high tissues more intensely for proteoglycan 4 (lubricin). This study demonstrated that FPSCs respond to joint-like environmental conditions by producing cartilage tissues mimicking native AC.

1
2
3
4
5
6
7
8
9
10
11
12
13
14
15
16
17
18
19
20
21
22
23
24
25
26
27
28
29
30
31
32
33
34
35
36
37
38
39
40
41
42
43
44
45
46
47
48
49
50
51
52
53
54
55
56
57
58
59
60

Keywords:

Cartilage tissue engineering, Oxygen, Mechanical environment, Confinement, Dynamic

compression, Proteoglycan 4.

1. Introduction

Articular cartilage (AC) is a highly organised tissue with spatially-varying structure and composition, which is typically divided into three distinct zones: the superficial, middle and deep zone. The cellular morphology, collagen network structure, and extracellular matrix (ECM) composition all vary through the depth of the tissue (Klein *et al.*, 2009a, Klein *et al.*, 2009b, Mow and Guo, 2002). For example, in human adult AC, the collagen content (as a % of dry weight) is highest in the superficial zone and decreases with depth, whereas glycosaminoglycan (GAG) content (as a % of dry weight) is lowest in the superficial zone and increases with depth (Muir *et al.*, 1970). This unique depth dependent structure and composition is crucial to the mechanical functions of AC (Roth and Mow, 1980, Williamson *et al.*, 2003, Wilson *et al.*, 2007, Gannon *et al.*, 2012, Gannon *et al.*, 2015a, Gannon *et al.*, 2015b). The high collagen content and its densely packed parallel structure in the superficial zone imparts substantial tensile strength to the tissue (Roth and Mow, 1980, Williamson *et al.*, 2003). It may also contribute to the low permeability observed in the superficial zone of AC (Mansour and Mow, 1976, Maroudas *et al.*, 1968), with removal of this collagen rich region significantly impacting the dynamic properties of the tissue (Gannon *et al.*, 2012, Gannon *et al.*, 2015a). Furthermore, the higher GAG content within the deeper regions of the tissue is also believed to contribute to the increases in compressive modulus with depth through AC (Schinagl *et al.*, 1997, Wilson *et al.*, 2007, Klein *et al.*, 2007).

Despite the importance of this zonal structure and composition to the functionality of AC, to date few studies have attempted to engineer tissues with a depth dependent

structure and composition mimicking that of AC. Previous studies have explored isolating chondrocytes from different zones of AC and incorporating them into specific regions of a hydrogel in order to engineer zonal cartilage tissue (Kim *et al.*, 2003, Klein *et al.*, 2003, Sharma *et al.*, 2007). While conceptually promising, difficulties distinguishing the different zones of AC when isolating cells from a diseased joint and the limited availability of zonal chondrocytes may limit the clinical translation of this approach (Klein *et al.*, 2009a). Other zonal tissue engineering strategies include varying the stiffness (Ng *et al.*, 2005, Ng *et al.*, 2006, Ng *et al.*, 2009) or composition (Nguyen *et al.*, 2011b) through the depth of a scaffold or hydrogel in an attempt to engineer zone specific environments. For example, Nguyen *et al.* demonstrated that unique biomaterial compositions can direct bone marrow derived mesenchymal stem cells (BMSCs) into specific chondrocytic phenotypes corresponding to the various zones of AC (Nguyen *et al.*, 2011a), and by incorporating these different biomaterial compositions into a tri-layered hydrogel that it was possible to engineer a tissue with spatially-varying mechanical and biochemical properties similar to native AC (Nguyen *et al.*, 2011b).

A potential limitation with such approaches is the development of engineered constructs consisting of specific (and homogenous) regions with distinct boundaries, as opposed to the creation of tissues with gradients in structure, composition and biomechanics mimicking the native tissue. An alternative approach to engineering zonal AC grafts is to recapitulate aspects of the tissue microenvironments which may be responsible for the formation of the zonal structure and composition in AC during tissue development and maturation (Thorpe *et al.*, 2013). In the case of articular

cartilage, low oxygen levels and mechanical stimulation are two joint specific environmental factors known to regulate chondrogenesis and cartilage tissue formation. Physiologically AC exists in a low oxygen environment, with the oxygen tension decreasing with depth from the articular surface (Zhou *et al.*, 2004). Furthermore, the tissue experiences various mechanical stimuli such as high magnitude cyclic hydrostatic pressure and distortional strains during joint movement (Mow and Guo, 2002). We have previously shown that it is possible to create AC-like gradients in oxygen levels through the depth of BMSC laden hydrogels by radial confinement of the developing constructs. When confinement was coupled with the application of dynamic compression, which produced a gradient in mechanical cues through the depth of these constructs, it was possible to engineer tissues with zonal gradients in biochemical composition mimicking certain aspects of native AC (Thorpe *et al.*, 2013). However the bulk tissue composition and mechanical properties of the engineered grafts were still inferior to the native tissue.

We and others have demonstrated that joint tissue derived stem cells, such as synovial membrane derived stem cells and infrapatellar fat pad derived stem cells (FPSCs), have a unique capacity for chondrogenesis (De Bari *et al.*, 2001, English *et al.*, 2007, Buckley *et al.*, 2010b, Vinardell *et al.*, 2012b, Vinardell *et al.*, 2012a, Carroll *et al.*, 2014), and can be used to engineer cartilage grafts with a bulk composition and mechanical properties approaching that of native tissue (Mesallati *et al.*, 2014). The hypothesis of this study is that joint tissue derived stem cells will generate AC-like tissue, both in terms of absolute levels of matrix accumulation and its spatial distribution, when presented with an environment mimicking that found through the depth of AC. To test

1
2
3
4
5
6
7
8
9
10
11
12
13
14
15
16
17
18
19
20
21
22
23
24
25
26
27
28
29
30
31
32
33
34
35
36
37
38
39
40
41
42
43
44
45
46
47
48
49
50
51
52
53
54
55
56
57
58
59
60

this hypothesis, FPSC laden hydrogels either 2mm or 4mm in height (spanning the cartilage thicknesses observed in large joints) were fabricated. Constructs were first cultured in a chondrogenic medium in unconfined free swelling conditions for 3 weeks, after which they were radially confined to half their thickness and subjected to dynamic compression for another 3 weeks. Finite element models were developed to predict the effects of these boundary conditions on nutrient availability (oxygen and glucose) and the mechanical environment within the developing constructs. The impact of these altered boundary conditions on the bulk and spatial development of the engineered grafts was also assessed.

2. Materials and Methods

2.1. Cell Isolation and Expansion

Porcine FPSCs were isolated from the entire IFP of the knee joint of the animal (3-4 months old, ~50kg) using a previously described protocol (Buckley and Kelly, 2012). Cells were seeded at a density of $5x10^3$ cell/cm^2 in high-glucose Dulbecco's modified Eagle's medium (hgDMEM) GlutaMAX^{TM} supplemented with 10% fetal bovine serum and 1% penicillin (100 U/mL)-streptomycin (100 µg/mL) (all GIBCO, Biosciences, Dublin, Ireland) and expanded to passage 2 in a humidified atmosphere of 5% CO_2 at 37°C. Fibroblast-growth factor-2 (ProSpec-Tany TechnoGene Ltd, Israel) was added during the whole expansion period at a concentration of 5 ng/ml to promote the growth and chondrogenic potential of the FPSCs (Buckley and Kelly, 2012).

2.2. Hydrogel construct fabrication and culture

At the end of passage 2, cells were harvested and encapsulated in agarose (Type VII, Sigma-Aldrich) as previously described (Thorpe *et al.*, 2010) to obtain a final gel concentration of 2% and a cell density of 20 x 10^6 cells/ml. The agarose-gel suspension was then cast between stainless steel plates, one of which was overlaid with a patterned polydimethylsiloxane layer, allowed cool to room temperature (RT), and cored to produce cylindrical constructs with a diameter of 6mm and a height of either 2mm or 4mm. All constructs were patterned on one surface. Both types of constructs (2mm/4mm height) were maintained in a 58 cm^2 culture dish (6 constructs per dish;

Nunclon; Nunc, VWR, Dublin, Ireland) in either 6 ml (per 2mm height constructs) or 9

ml (per 4mm height constructs) of chondrogenic medium consisting of hgDMEM

GlutaMAX^{TM} supplemented with penicillin (100 U/ml)-streptomycin (100 µg/ml), 100

µg/ml sodium pyruvate, 40 µg/ml L-proline, 4.7 µg/mL linoleic acid, 50 µg/ml L-

ascorbic acid-2-phosphate, 1.5 mg/ml bovine serum albumin, 1 × insulin–transferrin–

selenium, 100 nM dexamethasone (all from Sigma-Aldrich, Dublin, Ireland) and 10

ng/ml recombinant human transforming growth factor-β3 (TGF-β3; ProSpec-Tany

TechnoGene Ltd). Care was taken to ensure that the constructs remained patterned

surface up throughout the culture period and that they did not flip over to maintain

stable oxygen and glucose gradients within them. Media was exchanged twice weekly.

At each exchange media was sampled and stored at -85°C for biochemical analysis.

2.3.   *Experimental design*

Both 2mm and 4mm high constructs were first maintained in unconfined free swelling

(UFS) conditions in a chondrogenic medium for 21 days to allow matrix establishment

(Haugh *et al.*, 2011). At this point, samples were radially confined to half of their height

using custom made polytetrafluoroethylene confinement chambers and subjected to

cyclic dynamic compression of 10% strain (1Hz, 2 hours/day, 5 days/week) for a further

21 days as previously described (Thorpe *et al.*, 2013) (see CDC group; Fig. 1), while

samples remained in UFS conditions were used as a control. The effect of these

boundary conditions was to lower the oxygen tension in the bottom of the construct

and increase the magnitude of strain in the top of the tissue to more closely

recapitulate the microenvironment within articular cartilage. Samples that were confined but still in FS conditions (CFS) and samples that remained unconfined but subjected to DC (UDC) were also maintained to study the effects of confinement alone and dynamic compression alone on the development of the tissue (Fig. 1). Constructs (n=6 per group) were assessed at day 0, 21 and 42.

2.4. Computational modelling of oxygen and glucose transport

The diffusion of oxygen and glucose was modelled using a mass balance relation combined with Fick's law for diffusion (Sengers *et al.*, 2005, Thorpe *et al.*, 2013, Zhou *et al.*, 2004). The reaction term in the equation followed Michaelis-Menten kinetics:

$$\frac{\partial c}{\partial t} = D\nabla^2 c - n\frac{Q_m c}{K_m + c}$$

Here, c is the solute concentration [mol L^{-1}], D is the diffusion coefficient [cm^2 s^{-1}], n is the cell density [cells L^{-1}], Q_m is the maximum consumption rate [mol h^{-1}] and K_m is the concentration at half the maximum consumption rate [mol L^{-1}]. The values of the parameters for each solute diffusion model were obtained from the literature. For the oxygen model; Q_m (O_2) = 38.88 fmol h^{-1} cell^{-1} (Buckley *et al.*, 2012) and K_m (O_2) = 6 x 10^{-6} mol m^{-3} (Sengers *et al.*, 2005). Similarly, for the glucose diffusion model; Q_m (glucose) = 61.2 fmol h^{-1} cell^{-1} and K_m (glucose) = 0.35 x 10^{-3} mol m^{-3} (Sengers *et al.*, 2005). For both models the diffusion coefficient in 2 % agarose was calculated using the Mackie and Meares relation:

$$\frac{D_{agarose}}{D_{H_2 0}} = \frac{n_f^2}{(2 - n_f)}$$

Assuming that n_f = 0.98 for 2 % agarose. For the oxygen model, $D_{H20}(O_2)$ = 3.0 x 10^{-5} cm^2 s^{-1}, $D_{agarose,}(O_2)$ = 2.77 x 10^{-5} cm^2 s^{-1}. Similarly, for the glucose model, D_{H20} (glucose) = 0.92 x 10^{-5} cm^2 s^{-1} and $D_{agarose,}$ (glucose) = 0.85 x 10^{-5} cm^2 s^{-1}.

Using COMSOL, an axisymmetric model was constructed for both the confined and the unconfined case. In accordance with the experimental procedure, both groups were initially modelled as unconfined for the first 21 days, before being divided into their respective groups for the remaining 21 days. The initial value for glucose in the media was 25 mM, while for the oxygen model the initial value in the media was 208.5 µM; a value which corresponded to an oxygen tension of 21%. For the oxygen model there was also an essential boundary condition of 208.5 µM at the free surface to account for the diffusion of oxygen into the media from the atmosphere. A media change was modelled every 3.5 days at which point the oxygen and glucose concentrations in the media were returned to their initial values.

2.5.   Modelling of the mechanical environment within developing constructs

The peak fluid pressure and the strains in the engineered tissues were estimated during dynamic compression for both the confined and unconfined groups at day 21. Using the finite element package FEBio, a pseudo axisymmetric model was developed for both construct geometries, each of which were compressed to 10 % strain over 0.5 seconds. In order to characterise the heterogeneous distribution of collagen and GAG

through the construct, an algorithm was developed that used histological sections of

the engineered tissues to estimate the material parameters in each element of the

model based on its pixel intensity relative to the total number of pixels in the image.

Briefly, alcian blue and picrosirius red histology images were used to quantify the

spatial distribution of GAG and collagen, respectively, within the engineered tissues.

The algorithm involved dividing each image into elements corresponding to the mesh

of the finite element model. The relative pixel intensity was then used to determine

the percentage wet weight of the ECM component in each element of the image,

based on knowing the overall GAG and collagen content at that timepoint. The

mechanical properties of each element within the finite element model were then

updated with respect to the ECM concentration. The model parameters relating to

GAG levels were updated using a previously developed algorithm (Narmoneva *et al.*,

1999, Khoshgoftar *et al.*, 2012), while the material parameters related to the collagen

were changed using a simple linear approach outlined by Nagel *et al*. (Nagel and Kelly,

2012).

The governing stress equation in the model was similar to that used previously in the

literature (Nagel and Kelly, 2012), with the exception that fluid pressurization during

loading was also considered. Fluid pressure was accounted for as described previously

(Holmes and Mow, 1990). The total stress was thus given by:

$$\sigma_{total} = -\Delta\pi I + \sigma_{collagen} + \sigma_{agarose} - \mathrm{p}I$$

Here $\Delta\pi$ was the Donnan osmotic pressure which was dependent on the concentration

of GAG in the element; σ_{fibres} was the stress in the collagen fibre network, this was

assumed to be isotropic and dependent on the concentration of collagen in the element; $\sigma_{agarose}$ was the stress in the agarose hydrogel which was constant and isotropic; p represents the fluid pressure.

The method was validated by using it to predict the stress relaxation curve of the unconfined compression tests conducted at day 21 on the 2mm and 4mm constructs (see below). Both cases produced curves which matched the experimental data with an $R^2 > 0.95$.

2.6. Assessment of mechanical properties

Construct mechanical properties were tested (n=3/4 per group) using a standard materials testing machine with a 5N load cell (Zwick Roell Z005, Herefordshire, UK) as previously described (Buckley *et al.*, 2009). Briefly, constructs were immersed in phosphate buffered saline (PBS) bath and placed between two impermeable platens. A preload of 0.01 N was used to ensure direct contact between construct and platen surfaces. An unconfined stress-relaxation test was then performed, which consisted of a ramp compression up to 10% strain of the sample thickness followed by a hold period of 30 minutes until equilibrium was reached. The equilibrium compressive modulus of the sample was calculated from the equilibrium force. A dynamic test consisting of a cyclic strain amplitude of 1% at 1 Hz for 10 cycles was performed directly after the equilibrium test to determine the dynamic modulus.

2.7.   Quantitative biochemical analysis

After mechanical testing, constructs were maintained in PBS for 30 mins to allow them to recover to their initial thickness, after which constructs (n=3/4 per group) were transversely sliced into two halves for determination of the spatial distribution of matrix within the engineered tissue. The top and bottom halves of the samples were weighed (wet) and stored separately at -85 °C for subsequent analyses. Samples were digested with 125 µg/ml papain in 0.1 M sodium acetate, 5 mM L-cysteine HCl, 0.05 M EDTA, pH 6.0 (all Sigma-Aldrich) under constant rotation at 60 °C for 18 hours. The DNA content of the samples was measured using the Hoechst bisBenzimide H33258 dye assay with calf thymus DNA as a standard as previously described (Kim *et al.*, 1988). GAG content was quantified using the dimethylmethylene blue dye-binding assay (Blyscan, Biocolor Ltd., Northern Ireland), with a glycosaminoglycan standard. Collagen content was determined through measurement of the hydroxyproline content (Kafienah and Sims, 2004) and calculated using a hydroxyproline-to-collagen ratio of 1:7.69 (Ignat'eva *et al.*, 2007). GAG and collagen accumulation within constructs was normalized to construct wet weight and to DNA content. GAG and collagen release into the media during the whole culture period was also analysed using the methods described above. Total GAG and collagen synthesis was calculated as the sum of GAG and collagen accumulated within constructs and released into the media.

2.8.   Histology and immunohistochemistry

1
2
3
4
5
6
7
8
9
10
11
12
13
14
15
16
17
18
19
20
21
22
23
24
25
26
27
28
29
30
31
32
33
34
35
36
37
38
39
40
41
42
43
44
45
46
47
48
49
50
51
52
53
54
55
56
57
58
59
60

Whole constructs (n=2 per group) were fixed with 4% paraformaldehyde (Sigma-Aldrich), wax embedded and sectioned perpendicularly to the disk surface at a thickness of 5 μm. Sections were stained histologically with 1% alcian blue 8GX in 0.1M HCl for GAG distribution and with picro-sirius red for collagen distribution (all Sigma–Aldrich). Sections were immunohistochemically stained for collagen type II using a mouse monoclonal collagen type II antibody (1:100; 1 mg/mL; Abcam) as previously described (Thorpe *et al.*, 2010). Constructs were also immunohistochemically stained for proteoglycan 4 (PRG4) expression with a mouse monoclonal antibody (1:50; 0.5 mg/mL; Novus Biologicals, Littleton, USA) using a modified protocol. Briefly, Sections were enzymatically treated with 1 mg/ml pronase (64072 PUK/g; Millipore Ireland, Cork, Ireland) in a humidified environment at 37 °C for 12 mins. Slides were then blocked with blocking buffers consisting of PBS containing 1% bovine serum albumin and 10% goat serum (all Sigma-Aldrich) for 2 hours at RT and sections were incubated with the primary antibody diluted in blocking buffer at 4 °C over night. After washing in PBS/0.05% Tween20 (Sigma–Aldrich), sections were blocked for peroxydase activity using hydrogen peroxide (Sigma–Aldrich), followed by an incubation for 1 hour in the secondary antibody, anti-mouse IgG biotin antibody produced in goat (1:133; 2 mg/mL; Sigma-Aldrich). Colour was developed using the Vectastain ABC kit followed by exposure to peroxidase DAB substrate kit (both Vector Laboratories, Peterborough, UK). Sections of porcine cartilage and ligament were used as positive and negative controls for collagen type II staining respectively. For PRG4 staining, cartilage (superficial zone) was used as positive control and cartilage without the addition of primary antibody was used as negative control.

2.9.   Statistical analysis

Statistics were performed using MINITAB 15.1 software (Minitab Ltd., Coventry, UK). A two-sample T-test was used for data sets containing only two groups. For data sets which contain more than two groups, a general lineal model for analysis of variance with Tukey's test for multiple comparisons was used. Significance was determined at $p<0.05$ and a trend towards significance was defined as $p<0.1$. All graphical results are presented as mean ± standard deviation.

3. Results

3.1.   Construct height determines the spatial development of tissue engineered cartilage

The availability of regulatory factors such as oxygen and glucose within engineered tissues will depend on the size of the cell seeded construct. Therefore we first sought to explore how the height of FPSC seeded agarose hydrogels would determine the availability of oxygen and glucose within the construct and hence the spatial development of the engineered tissue. Constructs either 2mm or 4mm in height were fabricated, and care was taken to ensure they did not flip over during the culture period to maintain a stable oxygen and glucose gradient within them. Finite element models predicted that a low oxygen microenvironment is created in the bottom core of 2mm hydrogels ($\sim$5% O_2, see red circle area), while even lower oxygen levels were predicted in the bottom of the 4mm gels, with an average oxygen tension of 1.2% across the bottom half (Fig. 2A). Models also predict sufficient and relatively homogeneously distributed glucose levels within both 2mm and 4mm samples, with no obvious difference observed between them (Fig. 2B). The 2mm constructs stained reasonably homogenously for GAG and collagen, while a larger core region staining less intensely for GAG and collagen was observed in the 4mm gels (Fig. 2C and D).

To further explore the spatial development of the engineered tissues they were sliced half way along their height and the biochemical content of the 'top' and 'bottom' of the engineered tissue was measured (Fig. 3). At day 42, significant cell proliferation occurred in both the 2mm and 4mm gels, with higher DNA content measured

compared to day 0 (data now shown). The DNA content was higher in the top of both

2mm and 4mm tissues compared to the corresponding bottom region of each

construct (p<0.05; Fig. 3A), indicating greater cell proliferation in this region of the

engineered tissue. There was a trend (p<0.1) towards greater GAG accumulation (as a

% of wet weight) in the bottom of the 2mm constructs (Fig. 3B), which was significant

(P<0.01) when GAG content was normalised to DNA content (Fig. 3D). Greater

(P<0.001) collagen accumulation (as a % of wet weight) was observed in the top of the

4mm constructs (Fig. 3C), however no significant difference was observed if collagen

content was normalised to DNA content (Fig. 3E).

3.2. *Modulating spatial oxygen and glucose availability within FPSC seeded hydrogels by partially confining the constructs alters matrix synthesis and the spatial development of the engineered tissue*

As a low oxygen environment is known to enhance chondrogenesis of stem cells

(Buckley *et al.*, 2010a, Meyer *et al.*, 2010), we next sought to determine how reducing

oxygen availability to the bottom of FPSC seeded hydrogels, by radially confining the

bottom half of the engineered tissue, would influence matrix synthesis and distribution

throughout the construct. We have previously shown that this approach can be used

to increase GAG accumulation within the bottom of BMSC seeded hydrogels (Thorpe *et

al.*, 2013). Confining the hydrogels was predicted to lower the oxygen tension in the

bottom of the 2mm and 4mm gels (Fig. 4, see red circles). It was also predicted to

increase oxygen levels in the top of the engineered tissue (the confinement chamber

moved the construct higher in the culture media and hence nearer the oxygen source), leading to the development of a steeper oxygen gradient through the depth of the construct. A reduction in glucose availability throughout the hydrogels was also predicted in both the 2mm and 4mm confined gels, nevertheless this reduced glucose level (~18mM) is still predicted to be sufficient to maintain viable cells in culture (Fig. 4). Partial confinement of free swelling (CFS) hydrogels was found to increase both total GAG and collagen synthesis (ECM accumulated in hydrogel and released into the media) in the 2mm gels compared to unconfined free swelling (UFS) controls (p<0.05), however no significant difference was observed when total GAG or collagen synthesis was normalised to DNA content (Fig. 5A and B). In the 4mm gels, partial confinement reduced total GAG synthesis and this was also significant when total GAG synthesis was normalised to DNA content (p<0.05; Fig. 5A). Looking at the spatial development of the engineered tissues, it was found that confinement increased the DNA and collagen content within the top of both 2mm and 4mm gels (p<0.05; Fig. 5C and E). This increase in collagen content was not significant when normalised to DNA content (Supplementary Fig. 1A). Furthermore, confinement increased GAG accumulation throughout the 2mm gels, but reduced GAG accumulation throughout the 4mm gels (p<0.05; Fig. 5D). Histologically, it appeared that confinement increased GAG accumulation around the bottom periphery of the gels (Supplementary Fig. 1B).

3.3. ***The development of tissue engineered cartilage subjected to dynamic compression depends on the height of the construct***

We and others have previously shown that the application of delayed dynamic compression (either alone or combined with shear stress) can enhance the development of cartilage grafts engineered using MSCs (Thorpe *et al.*, 2013, Huang *et al.*, 2010, Bian *et al.*, 2012, Li *et al.*, 2010). Hence, we next sought to determine how the application of delayed dynamic compression (DC) would influence the bulk and spatial development of engineered tissues of differing heights. After 3 weeks in unconfined free swelling (UFS) culture, 2mm and 4mm FPSC seeded hydrogels were subjected to DC. Model predictions of the mechanical environment due to DC showed a very low fluid pressure in both 2mm and 4mm unconfined dynamically compressed (UDC) gels (~0.02 MPa; Fig. 6A). A relatively homogenous mechanical environment was predicted through the depth of both 2mm and 4mm engineered tissues, with no remarkable difference in strain levels predicted between 2mm and 4mm gels (Fig. 6A). GAG and collagen accumulation within the construct increased in the 2mm UDC gels compared to UFS controls (p<0.05; Fig. 7A and B). In contrast, DC reduced GAG (p<0.05) and collagen (p<0.1) accumulation within the 4mm gels (Fig. 7A and B). The reduction in GAG accumulation in the 4mm gels could be partially explained by an increase in GAG release to the media (Fig. 7A). When normalised to DNA content, total (accumulated + released) GAG and collagen synthesis was not significantly affected by the application of DC in either the 2mm or the 4mm gels (Fig. 7A and B).

DC was found to significantly increase the DNA and GAG content in both the top and bottom of 2mm gels, and to significantly increase the collagen content in the top of the same gels (p<0.05; Fig. 7C, D and E). These differences were no longer significant when matrix levels were normalised to DNA content (Supplementary Fig. 2A).

Immunohistochemistry revealed enhanced type II collagen deposition at the superficial region of 2mm UDC gels (Supplementary Fig. 2B). The increased levels of matrix accumulation due to the application of loading translated into improvements in the mechanical properties of the engineered tissues. The equilibrium modulus of the 2mm UDC gels was found to be 95.3kPa, compared to 43.3kPa for the UFS controls. The dynamic modulus of the 2mm UDC gels was found to be 1452kPa, compared to 969kPa for the UFS controls (data not shown). In contrast to the 2mm gels, DC reduced GAG accumulation in both the top and bottom of the 4mm gels (p<0.05; Fig. 7D and Supplementary Fig. 2A). Histologically, 4mm UDC gels appeared similar to UFS controls, albeit that alcian blue staining appeared slightly more homogenous within UDC gels (Supplementary Fig. 2B).

3.4. ***Coupling partial confinement and dynamic compression can lead to the development of engineered cartilage with zonal features mimicking certain aspects of the native tissue***

Separately confinement and DC have been shown to generally enhance the development of 2mm gels, but were not necessarily beneficial to the development of 4mm gels. Therefore we were interested in exploring how the combination of both factors would influence the development of the engineered tissues. Partially confining the hydrogels was predicted to alter the mechanical environment in both 2mm and 4mm confined dynamically compressed (CDC) hydrogels, leading to a higher fluid pressure inside the constructs and a dramatically increased strain magnitude across

the top of the constructs (Fig. 6). Overall, there was no synergistic effect of coupling

confinement and DC on overall levels of matrix accumulation and mechanical

properties of the constructs compared to the application of confinement alone or DC

alone (data not shown). There was however some important differences in the zonal

development of CDC constructs compared to UFS controls and other previously

reported experimental groups. In both 2mm and 4mm gels, the combination of

confinement and DC was found to lead to the development of an engineered tissue

that spatially best resembled native articular cartilage. Collagen accumulation was

significantly greater in the top of 2mm CDC gels (p<0.05; Fig. 8C), which was not

observed in UFS controls (this was also not observed in UDC gels, see Fig. 7E, but was

found in CFS gels, see Fig. 5E). No significant difference was observed in GAG

accumulation between the top and bottom of 2mm CDC gels (Fig. 7B); however GAG

accumulation was higher in the top of 2mm CFS gels (see Fig. 5D), a non-native

gradient in matrix levels. When normalised to DNA levels, GAG synthesis was found to

be greater in the bottom of CDC gels compared to the top (p<0.05; Supplementary Fig.

3A).

A similar gradient in collagen and GAG accumulation was observed in the 4mm CDC

gels (Fig. 8B and C). In fact, while the combination of confinement and DC was not

beneficial to overall levels of matrix accumulation in the 4mm gels, it did lead to the

development of a tissue with a zonal composition perhaps best mimicking that of the

native tissue of all experimental groups. GAG/DNA trended higher (p<0.1) and

collagen/DNA was lower (p<0.001) in the bottom of the 4mm CDC constructs

compared to the top (supplementary Fig. 3), which was not observed in any other

group. Furthermore, the superficial region of both 2mm and 4mm CDC constructs best mimicked that of the native tissue, staining weakly for GAG and strongly for type II collagen (Fig. 9A and B). In addition, proteoglycan (PRG4) staining was stronger in the superficial region of 4mm CDC constructs compared to UFS controls (Fig. 9C) and indeed UDC constructs (data not shown).

4. Discussion

Engineering tissues with a structure and spatial composition mimicking those of native articular cartilage remains a challenge. This study examined if FPSCs can be used to engineer cartilage grafts with a bulk biochemical composition and a spatial distribution similar to the native tissue. FPSCs were encapsulated in agarose hydrogels to make constructs of either 2mm or 4mm in height, and constructs were subjected to partial confinement and/or DC. Confinement alone was predicted to significantly lower oxygen levels in the bottom of both 2mm and 4mm gels, increasing GAG and collagen accumulation in 2mm gels, but lowering GAG accumulation in 4mm gels. The influence of DC alone on chondrogenesis of FPSCs was found to also depend on the height of the gels: DC increased GAG and collagen accumulation in 2mm gels, but decreased GAG accumulation in 4mm gels. When confinement was coupled with DC, an altered mechanical environment within constructs was predicted, with increased strain magnitude observed in the top of both 2mm and 4mm CDC constructs. This correlated with an increase in total collagen accumulation and collagen type II deposition within the top of both 2mm and 4mm CDC gels compared to UFS controls. Furthermore, the superficial region of 2mm and 4mm CDC constructs stained weakly for GAG and strongly for collagen type II, with enhanced staining for PRG4 further observed in 4mm CDC gels, thus mimicking certain aspects of the zonal composition in articular cartilage. Although the engineered tissue did not quite achieve native levels of matrix accumulation (approaching 3% GAG and 2% collagen as a percentage of wet weight) and biomechanical function (approaching 100kPa for the equilibrium modulus), they

are of a similar order of magnitude and may have attained the necessary function and

zonal composition to thrive within a load bearing defect (Nagel and Kelly, 2013).

A low oxygen microenvironment (~5%) was predicted to develop in the bottom core of

2mm FPSC seeded UFS hydrogels (Fig. 2A), which correlated with higher GAG synthesis

(as indicated by GAG/DNA levels) in the bottom of the engineered tissue (Fig. 3D).

However, no significant difference in collagen synthesis at per cell level (collagen/DNA)

was found between the top and bottom of the tissue (Fig. 3E). We have previously

demonstrated increased GAG/DNA but not collagen/DNA levels in FPSC seeded

hydrogels cultured in 5% oxygen compared to 20% oxygen (Buckley *et al.*, 2010a). An

even lower oxygen tension was predicted in the bottom of 4mm UFS gels, with an

average oxygen concentration of 1.2% across the bottom half. However, it didn't affect

either GAG or collagen synthesis at per cell level in the bottom of the tissue (Fig. 3D

and E). This suggested that while a low oxygen environment (~5% oxygen) can

promote the chondrogenesis of the stem cells (Buckley *et al.*, 2010a, Meyer *et al.*,

2010), very low oxygen levels may not necessarily be beneficial for the development of

the tissue. Previous studies have reported significant decreases in cell metabolism and

proteoglycan synthesis when freshly-excised articular cartilage explants were cultured

at an oxygen tension <2% (Lee and Urban, 1997). Furthermore, more recent studies

have demonstrated that severe hypoxia supresses the capacity of MSCs to undergo

chondrogenesis (Cicione *et al.*, 2013). Significantly higher collagen accumulation was

observed in the top of the 4mm gels compared to the bottom (Fig. 3C), which may be

attributed to the higher cell proliferation in the top of these constructs (Fig. 3A). In

fact, greater cell proliferation was also observed in the top of all experimental groups

(2mm and 4mm CFS, UDC and CDC). This may be explained by the fact that the higher oxygen tension environment generated in the top of the gels promoted a more proliferative phenotype, as greater cell proliferation has been observed in adipose derived stem cells cultured at 20% oxygen compared to 5% oxygen (Wang *et al.*, 2005).

Partial confinement was found to reduce GAG accumulation in the 4mm gels, but to enhance GAG accumulation in the 2mm gels. This could be explained by the fact that the confinement had a more critical impact on oxygen availability in the 4mm gels, with the average oxygen tension predicted to decrease from 1.24% to 0.24% (anoxia) in the bottom of these constructs. Previous studies have reported significantly decreased matrix production of chondrocytes when they were cultured in anoxic conditions (oxygen tension <0.1%) (Grimshaw and Mason, 2000), and as discussed above, such low levels of oxygen availability may supress MSC chondrogenesis (Cicione *et al.*, 2013).

The development of tissue engineered cartilage subjected to DC was found to also depend on the height of the construct. In 2mm gels the application of DC was found to increase GAG and collagen accumulation and the mechanical functionality of the engineered graft, with a 2-fold increase in the equilibrium modulus of engineered tissues. It also led to increases in type II collagen deposition, particularly at the top surface of the engineered tissue. This suggests that the unique combination of mechanical cues and oxygen tension (Fig. 2A) in this region of the 2mm constructs preferentially supports collagen type II deposition. In contrast to the 2mm gels, the application of DC lead to a reduction in matrix accumulation in the 4mm gels (Fig. 7).

The reduction in GAG accumulation within the 4mm gels could be partially explained by increased GAG release to the media in response to mechanical loading (Fig. 7A). The fact that the radial surface area of the 4mm gels is twice that of the 2mm gels may partially explain why such GAG loss is higher in the thicker gels. The increased levels of matrix accumulation in the mechanically loaded 2mm gels appeared to be driven by increased cell proliferation in these constructs. There is on obvious explanation for why DC only enhanced cell proliferation in the thinner gels. The finite element model suggests that this is unlikely due to differences in the mechanical environment alone, as similar strain levels and very low fluid pressures ($\sim$0.02 MPa, physiological level is $\sim$10 MPa) are predicted in the 2mm and 4m gels (Fig. 6). This suggests a more complex interplay between nutrient availability and mechanical cues is regulating FPSC fate in the different gels.

Articular cartilage (AC) is characterised by its unique depth dependent composition. The collagen content is highest at the superficial zone and decreases with depth, while GAG content is lowest in the superficial zone and increases with depth (Muir *et al.*, 1970). This depth dependent composition together with the collagen network organisation is crucial to the biomechanical properties of the tissue (Roth and Mow, 1980, Williamson *et al.*, 2003, Wilson *et al.*, 2007, Gannon *et al.*, 2012, Gannon *et al.*, 2015a, Gannon *et al.*, 2015b). Subjecting FPSC seeded hydrogels to both confinement and DC appeared to lead to the development of an engineered tissue that best mimicked the depth dependant composition of native AC. While confinement led to greater collagen accumulation in the top of engineered tissues, mimicking the native tissue, it also led to greater GAG accumulation in the top of the 2mm gels (Fig. 5D and

E). However, by coupling confinement and DC it was possible to engineer a tissue where GAG levels were not higher in the top of the tissue but where collagen levels were (Fig. 8B and C). Furthermore, the superficial region of CDC constructs best resembled that of the native tissue (Fig. 9A and B). Of note was the finding that the combination of partial confinement and DC lead to increased PRG4 deposition at the top surface of the 4mm gels (Fig. 9C). PRG4 is a protein expressed by the cells in the superficial zone of AC, which is important for the boundary lubrication of this tissue. Mechanical loading has previously been shown to be a key stimulus for PRG4 deposition (Grad *et al.*, 2005, Nugent-Derfus *et al.*, 2007), with the results of this study suggesting that the specific combination of oxygen availability and mechanical stimulation within this region of the 4mm high constructs is enhancing production of this superficial zone protein.

In conclusion, this study provided new insights into how enviormental factors within the joint, such as oxygen levels and mechanical loading, may contribute to the development of the depth dependent changes in compostion within AC. We demonstrated that, by regulating the spatial environment through the depth of developing constructs, it is possible to engineer cartilage tissues with zonal compositions mimicking certain aspects of AC using FPSCs. The attained zonal composition may better equip the engineered tissue to achieve a long-term stable cartilage repair. Mimicking the complex collagen architecture of AC will be required to engineered grafts that truly mimic the depth dependent properties of the native tissue.
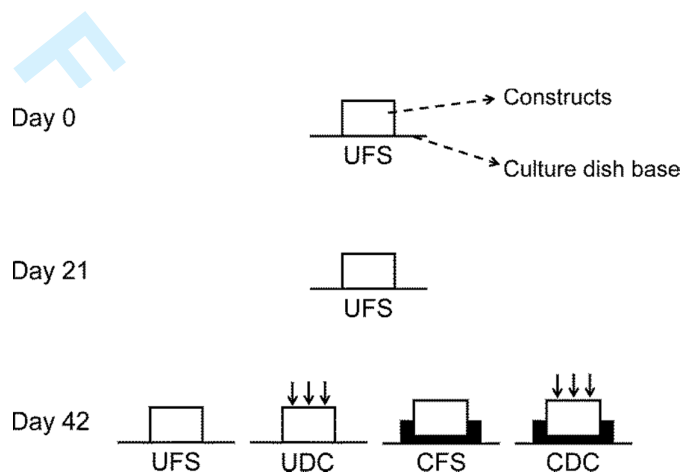
Acknowledgements

Figure 1. Experimental design. Constructs either 2mm or 4mm in height were first cultured in unconfined free swelling (UFS) conditions until day 21, and care was taken to ensure constructs did not flip over during the whole culture period to maintain a stable oxygen and glucose gradient within them. Samples were then confined to half of their height and subjected to dynamic compression (CDC) until day 42 while samples remained in UFS conditions were used as controls. Constructs that were confined but still in free swelling (CFS) conditions and constructs that remained unconfined but subjected to dynamic compression (UDC) were also maintained to study the effects of confinement alone and dynamic compression alone on the development of the tissue.
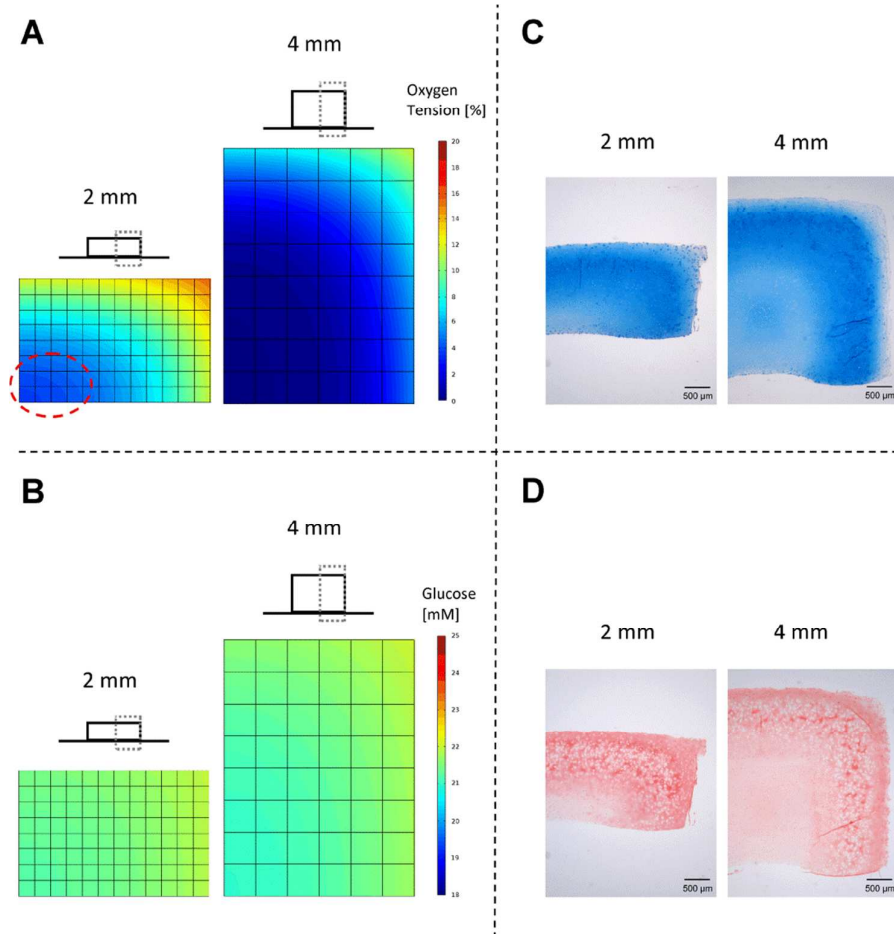
Figure 2. Oxygen and glucose environment and matrix distribution with 2mm and 4mm samples at day 42. (A) An axisymmetric computational model predicting oxygen environment and (B) an axisymmetric computational model predicting glucose environment within both 2mm and 4mm samples. The resulting oxygen/glucose concentration data was calculated from the regions within constructs which were indicated by grey boxes. (C) Alcian blue staining of GAG and (D) Picro-sirius red staining of collagen distribution within both samples at day 42. Histology images were taken at 2x magnification, and they represent approximately 2/3 of the whole sample.
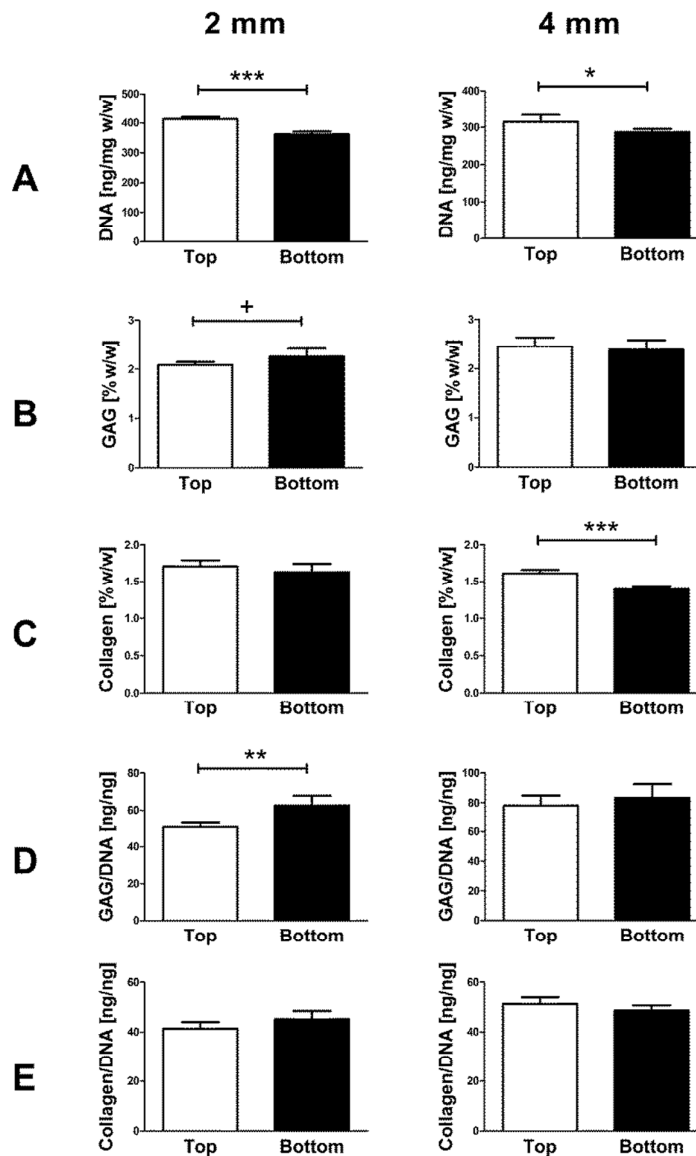
Figure 3. Biochemical content of the top and bottom halves of 2mm and 4mm unconfined free swelling (UFS) samples at day 42. (A) DNA content [ng/mg w/w]; (B) GAG content [% w/w]; (C) Collagen content [% w/w]; (D) GAG/DNA [ng/ng] and (E) Collagen/DNA [ng/ng]. +: trend, $p<0.1$; *: $p<0.05$; **: $p<0.01$; ***: $p<0.001$.
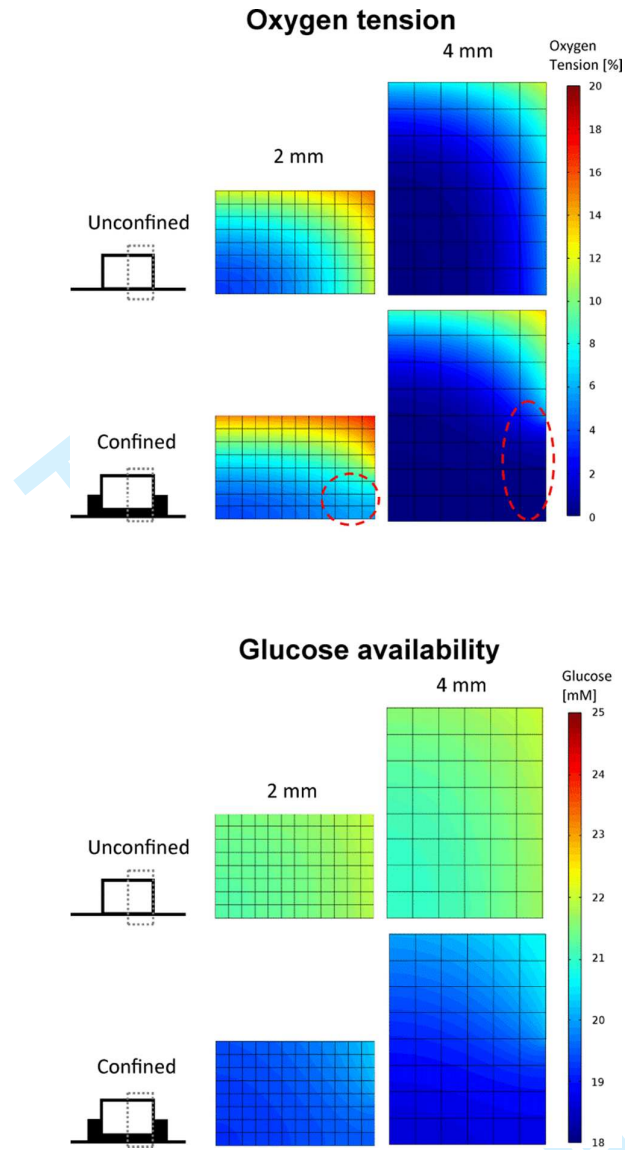
Oxygen tension

Glucose availability

Figure 4. An axisymmetric computational model predicting oxygen and glucose environment within unconfined and confined free swelling 2mm and 4mm samples at day 42. The resulting oxygen/glucose data was calculated from regions within constructs which were indicated by grey boxes. Red circles highlight regions with lowered oxygen tension in the 2mm and 4mm confined samples.
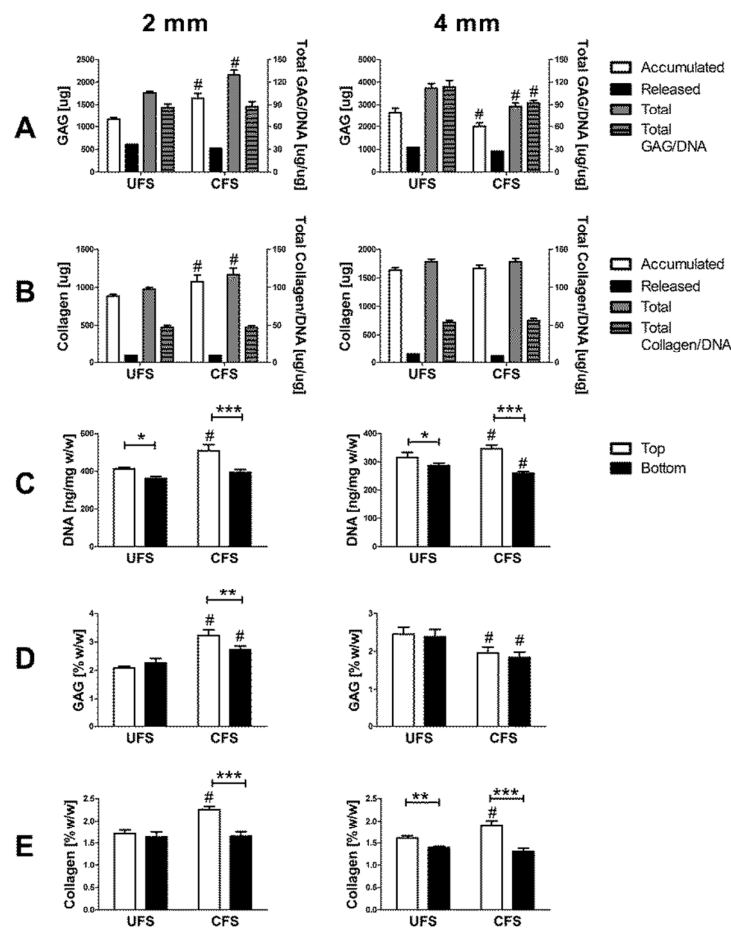
Figure 5. (A) GAG content [μg] and (B) collagen content [μg] accumulated within constructs, released into media and total synthesised (accumulated+released) in unconfined free swelling (UFS) and confined free swelling (CFS) 2mm and 4mm constructs at day 42. Total GAG/DNA [μg/μg] and total collagen/DNA [μg/μg] value were also plotted on the right Y axis within each graph. (C) DNA content [ng/mg w/w], (D) GAG content [%w/w] and (E) collagen content [%w/w] of the top and bottom halves of the UFS and CFS 2mm and 4mm samples at day 42. #: $p<0.05$ vs. UFS; *: $p<0.05$; **: $p<0.01$; ***: $p<0.001$.
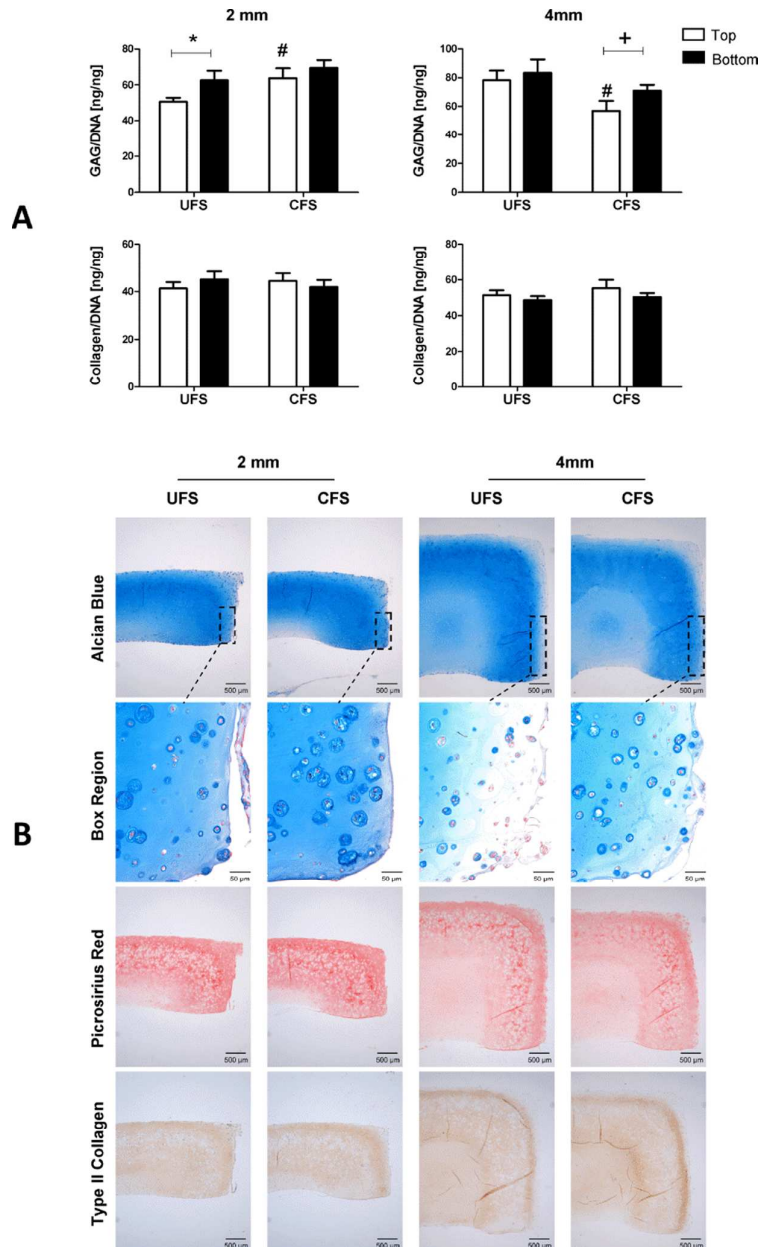
Supplementary figure 1. (A) GAG/DNA [ng/ng] and collagen/DNA [ng/ng] value of the top and bottom halves of UFS and CFS 2mm and 4mm constructs at day 42. #: $p < 0.05$ vs. UFS; +: trend, $p < 0.1$; *: $p < 0.05$. (B) Alcian blue, picrosirius red and collagen type II staining of UFS and CFS 2mm and 4mm constructs at day 42.
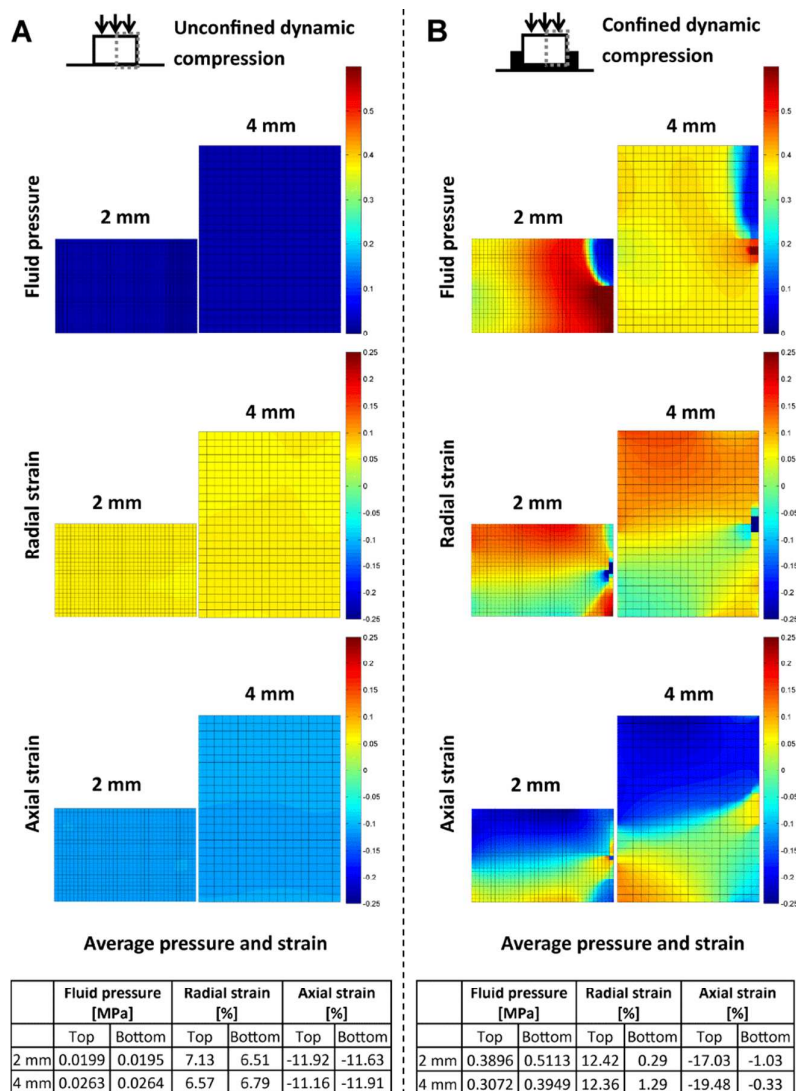
Average pressure and strain (A — Unconfined dynamic compression)

	Fluid pressure [MPa]		Radial strain [%]		Axial strain [%]	
	Top	Bottom	Top	Bottom	Top	Bottom
2 mm	0.0199	0.0195	7.13	6.51	-11.92	-11.63
4 mm	0.0263	0.0264	6.57	6.79	-11.16	-11.91

Average pressure and strain (B — Confined dynamic compression)

	Fluid pressure [MPa]		Radial strain [%]		Axial strain [%]	
	Top	Bottom	Top	Bottom	Top	Bottom
2 mm	0.3896	0.5113	12.42	0.29	-17.03	-1.03
4 mm	0.3072	0.3949	12.36	1.29	-19.48	-0.33

Figure 6. An axisymmetric computational model predicting the mechanical environment of fluid pressure [MPa], radial strain [%, positive] and axial strain [%, negative] within (A) unconfined dynamically compressed (UDC) and (B) confined dynamically compressed (CDC) 2mm and 4mm constructs at day 21. The mechanical environment data were calculated from regions within constructs, which were indicated by grey boxes.
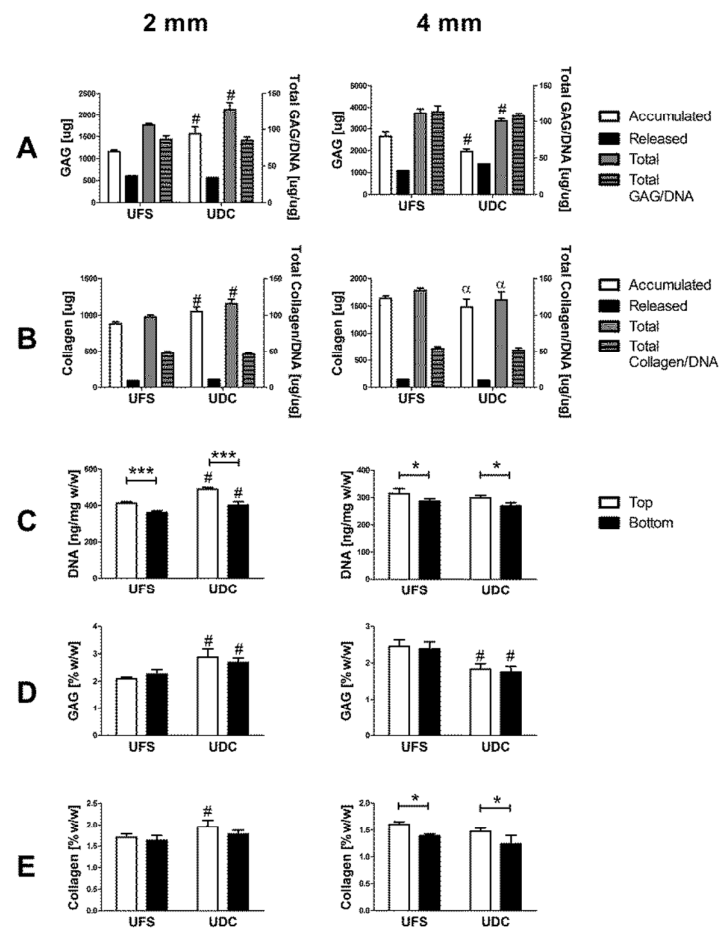
Figure 7. (A) GAG content [μg] and (B) collagen content [μg] accumulated within

constructs, released into media and total synthesised (accumulated+released) in

unconfined free swelling (UFS) and unconfined dynamically compressed (UDC) 2mm

and 4mm constructs at day 42. Total GAG/DNA [μg/μg] and total collagen/DNA [μg/μg]

value were also plotted on the right Y axis within each graph. (C) DNA content [ng/mg

w/w], (D) GAG content [%w/w] and (E) collagen content [%w/w] of the top and bottom

halves of the UFS and UDC 2mm and 4mm samples at day 42. α: trend, p<0.1 vs. UFS; #:

p<0.05 vs. UFS; *: p<0.05; ***: p<0.001.
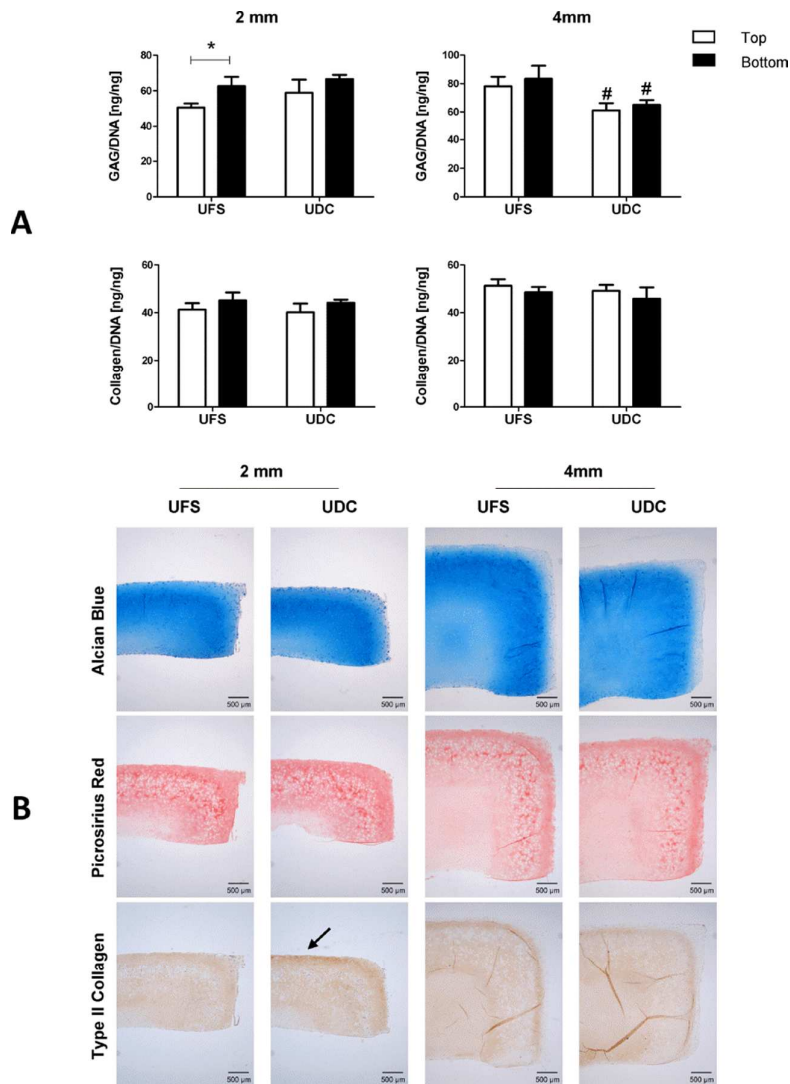
Supplementary figure 2. (A) GAG/DNA [ng/ng] and collagen/DNA [ng/ng] value of the top and bottom halves of UFS and UDC 2mm and 4mm constructs at day 42. #: $p<0.05$ vs. UFS; *: $p<0.05$. (B) Alcian blue, picrosirius red and collagen type II staining of UFS and UDC 2mm and 4mm constructs at day 42. Arrow indicates the enhanced collagen type II deposition in the superficial region of 2mm UDC constructs.
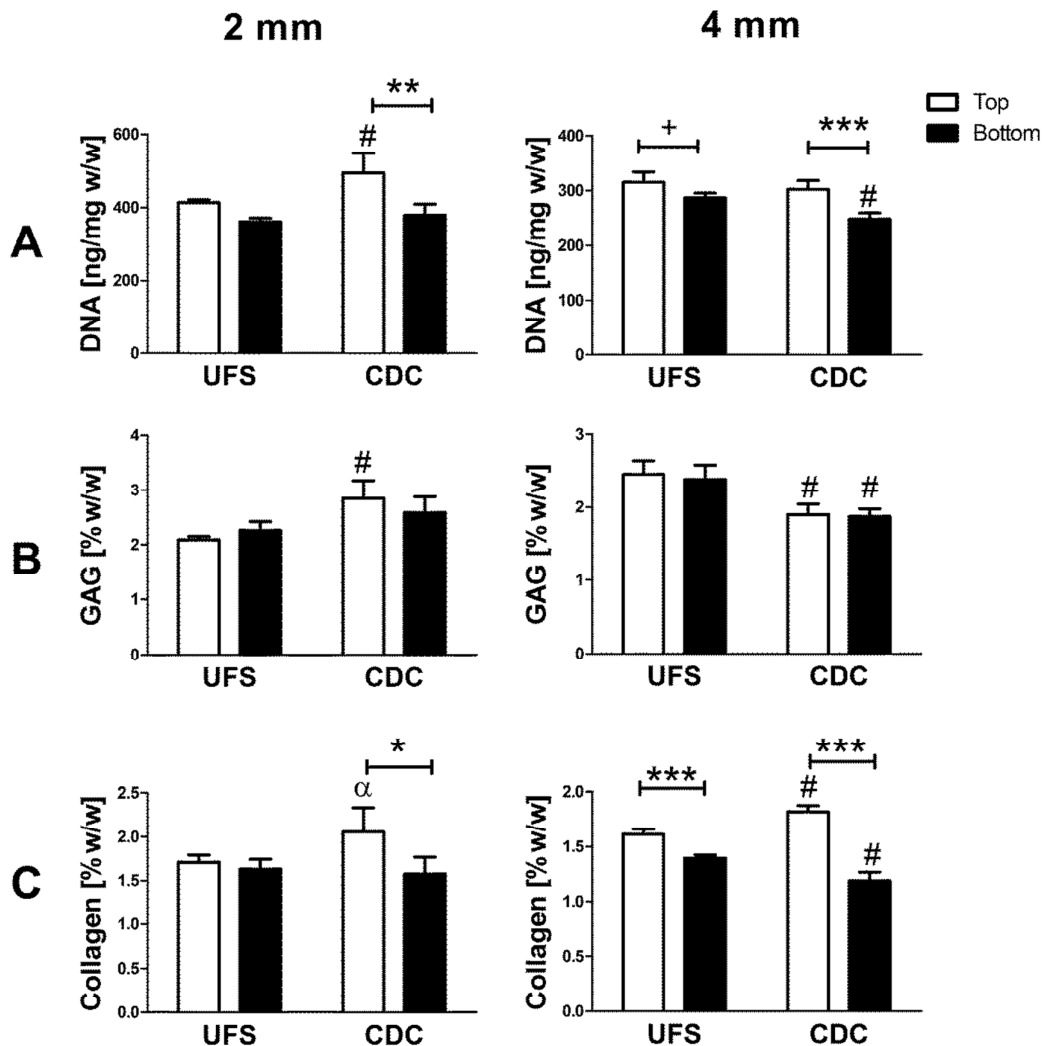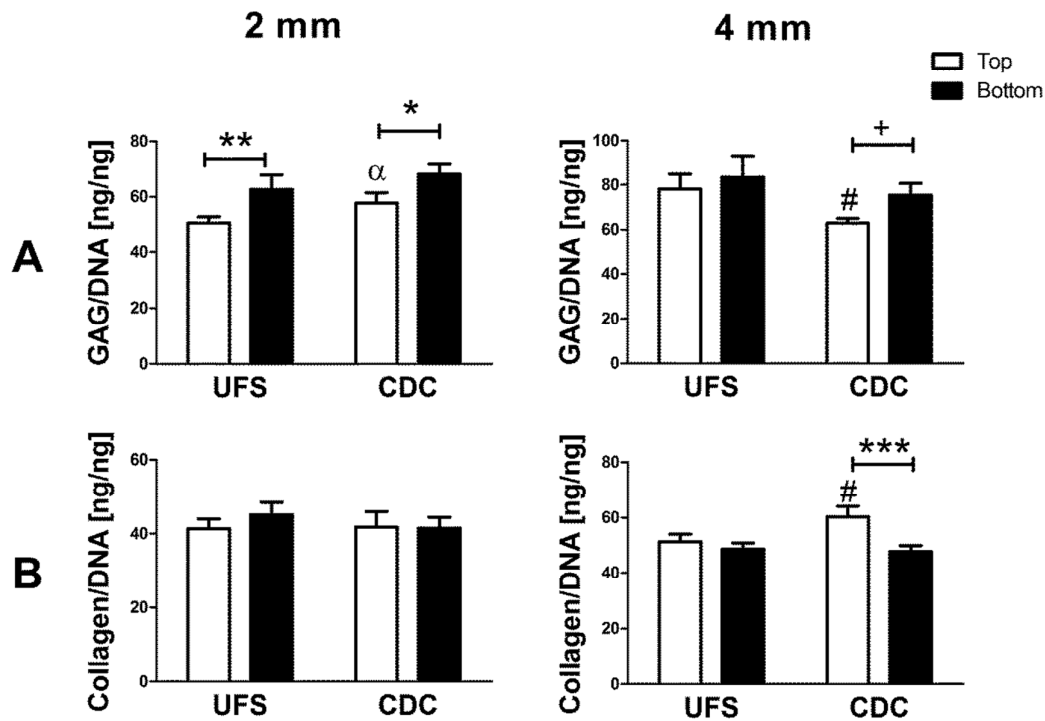
Figure 8. (A) DNA content [ng/mg w/w], (B) GAG content [%w/w] and (C) collagen

content [%w/w] of the top and bottom halves of the unconfined free swelling (UFS)

and confined dynamically compressed (CDC) 2mm and 4mm samples at day 42. α:

trend, p<0.1 vs. UFS; #: p<0.05 vs. UFS; +: trend, p<0.1; *: p<0.05; **: p<0.01; ***:

p<0.001.

Supplementary figure 3. (A) GAG/DNA [ng/ng] and (B) collagen/DNA [ng/ng] value of the top and bottom halves of UFS and CDC 2mm and 4mm constructs at day 42. α: trend, p<0.1 vs. UFS; #: p<0.05 vs. UFS; +: trend, p<0.1; *: p<0.05; **: p<0.01; ***: p<0.001.
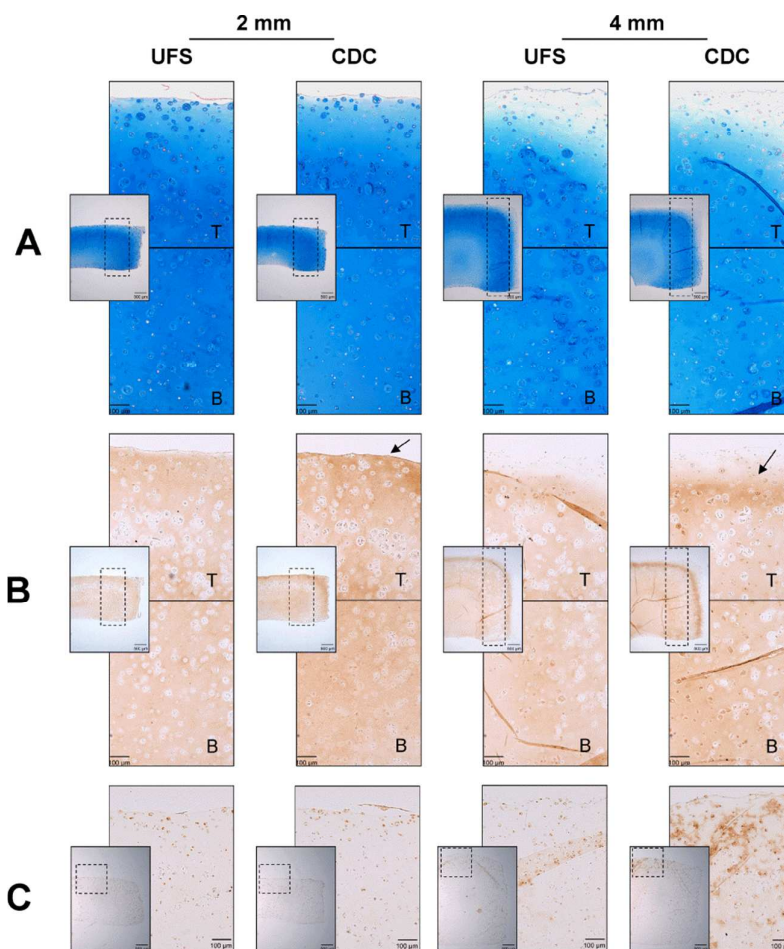
Figure 9. (A) Alcian blue staining for GAG distribution and (B) Immunohistochemical staining for collagen type II distribution through the depth of UFS and CDC 2mm and 4mm constructs at day 42. T: top; B: bottom. Inserted images were taken at 2x magnification to show staining at bulk construct level, with box regions indicating areas where high magnification images were taken. Arrows indicate the enhanced collagen type II deposition in the superficial region of both 2mm and 4mm CDC constructs. (C) Immunohistochemical staining for PRG4 expression at the superficial region of UFS and CDC 2mm and 4mm constructs at day 42.

Reference

Bian L, Zhai DY, Zhang EC *et al.* 2012, Dynamic compressive loading enhances cartilage matrix synthesis and distribution and suppresses hypertrophy in hmsc-laden hyaluronic acid hydrogels, *Tissue Eng Part A,* 18: 715-724.

Buckley CT, Kelly DJ. 2012, Expansion in the presence of fgf-2 enhances the functional development of cartilaginous tissues engineered using infrapatellar fat pad derived mscs, *J Mech Behav Biomed Mater,* 11: 102-111.

Buckley CT, Meyer EG, Kelly DJ. 2012, The influence of construct scale on the composition and functional properties of cartilaginous tissues engineered using bone marrow-derived mesenchymal stem cells, *Tissue Eng Part A,* 18: 382-396.

Buckley CT, Thorpe SD, O'brien FJ *et al.* 2009, The effect of concentration, thermal history and cell seeding density on the initial mechanical properties of agarose hydrogels, *J Mech Behav Biomed Mater,* 2: 512-521.

Buckley CT, Vinardell T, Kelly DJ. 2010a, Oxygen tension differentially regulates the functional properties of cartilaginous tissues engineered from infrapatellar fat pad derived mscs and articular chondrocytes, *Osteoarthritis Cartilage,* 18: 1345-1354.

Buckley CT, Vinardell T, Thorpe SD *et al.* 2010b, Functional properties of cartilaginous tissues engineered from infrapatellar fat pad-derived mesenchymal stem cells, *J Biomech,* 43: 920-926.

Carroll SF, Buckley CT, Kelly DJ. 2014, Cyclic hydrostatic pressure promotes a stable cartilage phenotype and enhances the functional development of cartilaginous

grafts engineered using multipotent stromal cells isolated from bone marrow and infrapatellar fat pad, *J Biomech,* 47: 2115-2121.

Cicione C, Muinos-Lopez E, Hermida-Gomez T *et al.* 2013, Effects of severe hypoxia on bone marrow mesenchymal stem cells differentiation potential, *Stem Cells Int,* 2013: 232896.

De Bari C, Dell'accio F, Tylzanowski P *et al.* 2001, Multipotent mesenchymal stem cells from adult human synovial membrane, *Arthritis Rheum,* 44: 1928-1942.

English A, Jones EA, Corscadden D *et al.* 2007, A comparative assessment of cartilage and joint fat pad as a potential source of cells for autologous therapy development in knee osteoarthritis, *Rheumatology (Oxford),* 46: 1676-1683.

Gannon AR, Nagel T, Bell AP *et al.* 2015a, The changing role of the superficial region in determining the dynamic compressive properties of articular cartilage during postnatal development, *Osteoarthritis and Cartilage,* 23: 975-984.

Gannon AR, Nagel T, Bell AP *et al.* 2015b, Postnatal changes to the mechanical properties of articular cartilage are driven by the evolution of its collagen network, *European Cells and Materials,* 29: 105-123.

Gannon AR, Nagel T, Kelly DJ. 2012, The role of the superficial region in determining the dynamic properties of articular cartilage, *Osteoarthritis Cartilage,* 20: 1417-1425.

Grad S, Lee CR, Gorna K *et al.* 2005, Surface motion upregulates superficial zone protein and hyaluronan production in chondrocyte-seeded three-dimensional scaffolds, *Tissue Eng,* 11: 249-256.

Grimshaw MJ, Mason RM. 2000, Bovine articular chondrocyte function in vitro depends upon oxygen tension, *Osteoarthritis Cartilage,* 8: 386-392.

Haugh MG, Meyer EG, Thorpe SD *et al.* 2011, Temporal and spatial changes in cartilage-matrix-specific gene expression in mesenchymal stem cells in response to dynamic compression, *Tissue Eng Part A,* 17: 3085-3093.

Holmes MH, Mow VC. 1990, The nonlinear characteristics of soft gels and hydrated connective tissues in ultrafiltration, *J Biomech,* 23: 1145-1156.

Huang AH, Farrell MJ, Kim M *et al.* 2010, Long-term dynamic loading improves the mechanical properties of chondrogenic mesenchymal stem cell-laden hydrogel, *Eur Cell Mater,* 19: 72-85.

Ignat'eva NY, Danilov NA, Averkiev SV *et al.* 2007, Determination of hydroxyproline in tissues and the evaluation of the collagen content of the tissues, *Journal of Analytical Chemistry,* 62: 51-57.

Kafienah W, Sims TJ. 2004, Biochemical methods for the analysis of tissue-engineered cartilage, *Methods Mol Biol,* 238: 217-230.

Khoshgoftar M, Wilson W, Ito K *et al.* 2012, Influence of tissue- and cell-scale extracellular matrix distribution on the mechanical properties of tissue-engineered cartilage, *Biomech Model Mechanobiol*.

Kim TK, Sharma B, Williams CG *et al.* 2003, Experimental model for cartilage tissue engineering to regenerate the zonal organization of articular cartilage, *Osteoarthritis and Cartilage,* 11: 653-664.

Kim YJ, Sah RL, Doong JY *et al.* 1988, Fluorometric assay of DNA in cartilage explants using hoechst 33258, *Anal Biochem,* 174: 168-176.

Klein TJ, Chaudhry M, Bae WC *et al.* 2007, Depth-dependent biomechanical and biochemical properties of fetal, newborn, and tissue-engineered articular cartilage, *J Biomech,* 40: 182-190.

Klein TJ, Malda J, Sah RL *et al.* 2009a, Tissue engineering of articular cartilage with biomimetic zones, *Tissue Eng Part B Rev,* 15: 143-157.

Klein TJ, Rizzi SC, Reichert JC *et al.* 2009b, Strategies for zonal cartilage repair using hydrogels, *Macromol Biosci,* 9: 1049-1058.

Klein TJ, Schumacher BL, Schmidt TA *et al.* 2003, Tissue engineering of stratified articular cartilage from chondrocyte subpopulations, *Osteoarthritis and Cartilage,* 11: 595-602.

Lee RB, Urban JP. 1997, Evidence for a negative pasteur effect in articular cartilage, *Biochem J,* 321 (Pt 1): 95-102.

Li Z, Yao SJ, Alini M *et al.* 2010, Chondrogenesis of human bone marrow mesenchymal stem cells in fibrin-polyurethane composites is modulated by frequency and amplitude of dynamic compression and shear stress, *Tissue Eng Part A,* 16: 575-584.

Mansour JM, Mow VC. 1976, The permeability of articular cartilage under compressive strain and at high pressures, *J Bone Joint Surg Am,* 58: 509-516.

Maroudas A, Bullough P, Swanson S *et al.* 1968, The permeability of articular cartilage, *Journal of Bone & Joint Surgery, British Volume,* 50: 166-177.

Mesallati T, Buckley CT, Kelly DJ. 2014, Engineering articular cartilage-like grafts by self-assembly of infrapatellar fat pad-derived stem cells, *Biotechnol Bioeng,* 111: 1686-1698.

Meyer EG, Buckley CT, Thorpe SD *et al.* 2010, Low oxygen tension is a more potent

promoter of chondrogenic differentiation than dynamic compression, *J Biomech,* 43: 2516-2523.

Mow VC, Guo XE. 2002, Mechano-electrochemical properties of articular cartilage:

Their inhomogeneities and anisotropies, *Annu Rev Biomed Eng,* 4: 175-209.

Muir H, Bullough P, Maroudas A. 1970, The distribution of collagen in human articular

cartilage with some of its physiological implications, *J Bone Joint Surg Br,* 52: 554-563.

Nagel T, Kelly DJ. 2012, Apparent behaviour of charged and neutral materials with

ellipsoidal fibre distributions and cross-validation of finite element

implementations, *Journal of the mechanical behavior of biomedical materials,* 9: 122-129.

Nagel T, Kelly DJ. 2013, The composition of engineered cartilage at the time of

implantation determines the likelihood of regenerating tissue with a normal

collagen architecture, *Tissue Eng Part A,* 19: 824-833.

Narmoneva D, Wang J, Setton L. 1999, Nonuniform swelling-induced residual strains in

articular cartilage, *Journal of biomechanics,* 32: 401-408.

Ng KW, Ateshian GA, Hung CT. 2009, Zonal chondrocytes seeded in a layered agarose

hydrogel create engineered cartilage with depth-dependent cellular and

mechanical inhomogeneity, *Tissue Eng Part A,* 15: 2315-2324.

Ng KW, Mauck RL, Statman LY *et al.* 2006, Dynamic deformational loading results in

selective application of mechanical stimulation in a layered, tissue-engineered

cartilage construct, *Biorheology,* 43: 497-507.

Ng KW, Wang CC, Mauck RL *et al.* 2005, A layered agarose approach to fabricate depth-dependent inhomogeneity in chondrocyte-seeded constructs, *J Orthop Res,* 23: 134-141.

Nguyen LH, Kudva AK, Guckert NL *et al.* 2011a, Unique biomaterial compositions direct bone marrow stem cells into specific chondrocytic phenotypes corresponding to the various zones of articular cartilage, *Biomaterials,* 32: 1327-1338.

Nguyen LH, Kudva AK, Saxena NS *et al.* 2011b, Engineering articular cartilage with spatially-varying matrix composition and mechanical properties from a single stem cell population using a multi-layered hydrogel, *Biomaterials,* 32: 6946-6952.

Nugent-Derfus G, Takara T, O'neill J *et al.* 2007, Continuous passive motion applied to whole joints stimulates chondrocyte biosynthesis of prg4, *Osteoarthritis and cartilage,* 15: 566-574.

Roth V, Mow VC. 1980, The intrinsic tensile behavior of the matrix of bovine articular cartilage and its variation with age, *J Bone Joint Surg Am,* 62: 1102-1117.

Schinagl RM, Gurskis D, Chen AC *et al.* 1997, Depth-dependent confined compression modulus of full-thickness bovine articular cartilage, *J Orthop Res,* 15: 499-506.

Sengers BG, Van Donkelaar CC, Oomens CW *et al.* 2005, Computational study of culture conditions and nutrient supply in cartilage tissue engineering, *Biotechnol Prog,* 21: 1252-1261.

Sharma B, Williams CG, Kim TK *et al.* 2007, Designing zonal organization into tissue-engineered cartilage, *Tissue Eng,* 13: 405-414.

Thorpe SD, Buckley CT, Vinardell T *et al.* 2010, The response of bone marrow-derived mesenchymal stem cells to dynamic compression following tgf-beta3 induced chondrogenic differentiation, *Ann Biomed Eng,* 38: 2896-2909.

Thorpe SD, Nagel T, Carroll SF *et al.* 2013, Modulating gradients in regulatory signals within mesenchymal stem cell seeded hydrogels: A novel strategy to engineer zonal articular cartilage, *PLoS One,* 8: e60764.

Vinardell T, Rolfe RA, Buckley CT *et al.* 2012a, Hydrostatic pressure acts to stabilise a chondrogenic phenotype in porcine joint tissue derived stem cells, *Eur Cell Mater,* 23: 121-132; discussion 133-124.

Vinardell T, Sheehy EJ, Buckley CT *et al.* 2012b, A comparison of the functionality and in vivo phenotypic stability of cartilaginous tissues engineered from different stem cell sources, *Tissue Eng Part A,* 18: 1161-1170.

Wang DW, Fermor B, Gimble JM *et al.* 2005, Influence of oxygen on the proliferation and metabolism of adipose derived adult stem cells, *J Cell Physiol,* 204: 184-191.

Williamson AK, Chen AC, Masuda K *et al.* 2003, Tensile mechanical properties of bovine articular cartilage: Variations with growth and relationships to collagen network components, *J Orthop Res,* 21: 872-880.

Wilson W, Huyghe JM, Van Donkelaar CC. 2007, Depth-dependent compressive equilibrium properties of articular cartilage explained by its composition, *Biomech Model Mechanobiol,* 6: 43-53.

Zhou S, Cui Z, Urban JP. 2004, Factors influencing the oxygen concentration gradient

from the synovial surface of articular cartilage to the cartilage-bone interface: A

modeling study, *Arthritis Rheum,* 50: 3915-3924.